Enhanced limonene production in cyanobacteria reveals photosynthesis limitations

Xin Wang[a,b,c], Wei Liu[a,b,d], Changpeng Xin[e], Yi Zheng[a,b,f], Yanbing Cheng[b], Su Sun[b], Runze Li[g], Xin-Guang Zhu[e], Susie Y. Dai[b,h], Peter M. Rentzepis[b,g,1], and Joshua S. Yuan[a,b,c,1]

[a]Department of Plant Pathology and Microbiology, Texas A&M University, College Station, TX 77843; [b]Synthetic and Systems Biology Innovation Hub, Texas A&M University, College Station, TX 77843; [c]Institute for Plant Genomics and Biotechnology, Texas A&M University, College Station, TX 77843; [d]College of Life Science, Tonghua Normal University, Jilin 134002, People's Republic of China; [e]Key Laboratory of Computational Biology, Chinese Academy of Sciences (CAS)-German Max Planck Society (MPG) Partner Institute for Computational Biology, Shanghai Institutes of Biological Sciences, Chinese Academy of Sciences, Shanghai 200031, People's Republic of China; [f]College of Resource and Environmental Science, Fujian Agriculture and Forestry University, Fujian 350002, People's Republic of China; [g]Department of Electrical and Computer Engineering, Texas A&M University, College Station, TX 77843; and [h]Department of Veterinary Pathobiology, Texas A&M University, College Station, TX 77843

Contributed by Peter M. Rentzepis, November 3, 2016 (sent for review August 24, 2016; reviewed by James Moroney and Shihui Yang)

Terpenes are the major secondary metabolites produced by plants, and have diverse industrial applications as pharmaceuticals, fragrance, solvents, and biofuels. Cyanobacteria are equipped with efficient carbon fixation mechanism, and are ideal cell factories to produce various fuel and chemical products. Past efforts to produce terpenes in photosynthetic organisms have gained only limited success. Here we engineered the cyanobacterium *Synechococcus elongatus* PCC 7942 to efficiently produce limonene through modeling guided study. Computational modeling of limonene flux in response to photosynthetic output has revealed the downstream terpene synthase as a key metabolic flux-controlling node in the MEP (2-C-methyl-D-erythritol 4-phosphate) pathway-derived terpene biosynthesis. By enhancing the downstream limonene carbon sink, we achieved over 100-fold increase in limonene productivity, in contrast to the marginal increase achieved through stepwise metabolic engineering. The establishment of a strong limonene flux revealed potential synergy between photosynthate output and terpene biosynthesis, leading to enhanced carbon flux into the MEP pathway. Moreover, we show that enhanced limonene flux would lead to NADPH accumulation, and slow down photosynthesis electron flow. Fine-tuning ATP/NADPH toward terpene biosynthesis could be a key parameter to adapt photosynthesis to support biofuel/bioproduct production in cyanobacteria.

photosynthesis | limonene | advanced biofuel | terpene | MEP

Efficient carbon partition into desired molecules is a major scientific challenge in producing chemicals in photosynthetic organisms (1). Earlier approaches often involved overexpressing pathway enzymes to enhance carbon flux, but these approaches were hindered by the limited understanding of metabolic network and its regulation. In particular, many low-flux pathways (e.g., terpene biosynthesis) impede carbon partition due to metabolic rigidity (2, 3). Moreover, the importance and requirement of energy balance in improving photosynthetic productivity (4), is often neglected in engineering efforts. Recently, a few studies have demonstrated the possibility of producing terpenes in cyanobacteria, but the productivity is rather low (2, 5–7). Enhancing carbon flux into a low-flux terpene pathway could provide intuitive insight to both carbon partition and photosynthesis regulations. Through computational modeling, we show that downstream limonene synthase is a key flux-controlling node in the 2-*C*-methyl-D-erythritol 4-phosphate (MEP)-derived limonene biosynthesis in cyanobacteria. Overcoming this metabolic bottleneck led to a record limonene productivity in the engineered cyanobacteria. Moreover, we show that enhanced limonene production led to redox change and energy imbalance, which ultimately limit photosynthesis capacity. The study demonstrates a successful strategy to enhance carbon partition into MEP-derived terpene biosynthesis, and reveals key photosynthesis regulations in providing ATP/NADPH to support terpene production.

Stepwise Metabolic Engineering Is Limited in Enhancing Limonene Productivity

We first generated cyanobacterial strains to produce limonene through stepwise metabolic engineering. Terpenes are synthesized from two C_5 precursor molecules, isopentenyl pyrophosphate (IPP) and dimethylallyl pyrophosphate (DMAPP). In cyanobacteria, IPP and DMAPP are derived from the MEP pathway, where glyceraldehyde 3-phosphate (G3P) and pyruvate are condensed into the C_5 precursors through seven enzymatic steps (2) (Fig. 1*A*). Limonene synthase (LS) from spearmint (*Mentha spicata*) was chosen to generate limonene because of its high fidelity, i.e., >90% of LS product is limonene with minimal isomers (8). The protein sequence of native LS includes a signal peptide for its expression in plant chloroplasts. To enable heterologous expression, a truncated version of LS (9) was synthesized and codon-optimized for *Synechococcus elongatus* PCC 7942 (hereafter *S. elongatus*) expression driven by an isopropyl-β-D-thiogalactoside (IPTG) inducible promoter *P*trc. LS gene was then integrated into neutral site I of *S. elongatus* genome

Significance

Life on Earth depends on photosynthesis to capture solar energy and reduce CO_2 into organic carbons. One strategy to improve photosynthesis is to enhance carbon assimilation by "nonnative" carbon sinks (e.g., terpene biosynthesis). Previous attempts to enhance terpene biosynthesis in photosynthetic organisms have met with limited success. Through computational modeling and synthetic biology tools, we identified and overcame a key flux-controlling node in 2-C-methyl-D-erythritol 4-phosphate–derived terpene biosynthesis in cyanobacteria. This strategy bypasses the limitation in traditional stepwise metabolic engineering, and enables record limonene productivity. The breakthrough allowed systems biology analysis to reveal photosynthesis regulations under a high level of limonene production. Fine-tuning energy and reductant requirement could be a key factor to further synergize photosynthesis and terpene production.

Author contributions: X.W., P.M.R., and J.S.Y. designed research; X.W., W.L., Y.Z., and S.S. performed research; R.L., X.-G.Z., S.Y.D., P.M.R., and J.S.Y. contributed new reagents/analytic tools; X.W., C.X., Y.C., P.M.R., and J.S.Y. analyzed data; X.W. drafted the manuscript; and X.-G.Z., S.Y.D., P.M.R., and J.S.Y. revised the manuscript.

Reviewers: J.M., Louisiana State University; and S.Y., National Renewable Energy Laboratory.

The authors declare no conflict of interest.

Data deposition: Mass spectrometry proteomics data have been deposited in the ProteomeXchange Consortium via the PRIDE partner repository, proteomecentral.proteomexchange.org/cgi/GetDataset (dataset identifier PXD005105).

[1]To whom correspondence may be addressed. Email: prentzepis@tamu.edu or syuan@tamu.edu.

This article contains supporting information online at www.pnas.org/lookup/suppl/doi:10.1073/pnas.1613340113/-/DCSupplemental.

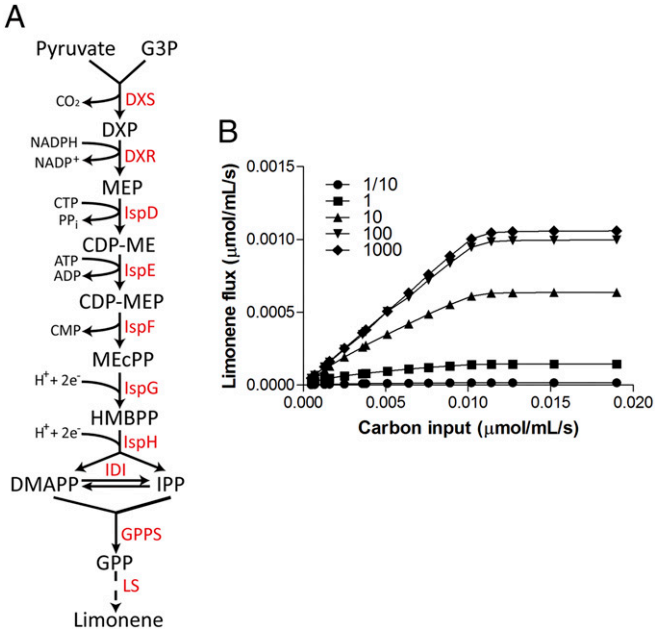

Fig. 1. Pathway modeling suggests LS as the key limiting step in cyanobacterial limonene production. (*A*) MEP pathway in cyanobacteria for generating IPP/DMAPP, which are further converted to downstream terpenes. (*B*) Kinetics modeling to simulate limonene flux in response to carbon input. The baseline LS kinetics was obtained from literature, and various fold changes in LS activity were simulated.

(10), creating strain L111. The engineered strain was able to produce limonene but at a low average productivity of 8.5 μg/L/OD/d (*SI Appendix*, Figs. S1 and S2). To enhance LS expression, a synthetic ribosomal binding site (RBS) sequence generated using an RBS calculator (11) was engineered into the *P*trc promoter for LS expression. Strain L113 in which LS expression was driven by *P*trc promoter with the synthetic RBS increased the limonene productivity to 32.8 μg/L/OD/d (*SI Appendix*, Fig. S1 and File S1). The enzyme ahead of terpene cyclase was shown to play important roles in directing precursors into the downstream terpene synthase in tobacco (12). A fir (*Abies grandis*) geranyl pyrophosphate synthase (GPPS) (13) was thus synthesized and codon optimized for *S. elongatus* expression, and coexpressed with LS in a single operon, yielding strain L114. Limonene productivity of L114 increased another fold to 65.4 μg/L/OD/d (*SI Appendix*, Fig. S1). DXS (1-deoxy-D-xylulose 5-phosphate synthase) is believed to be the flux-controlling point in the MEP pathway (14), and essential in metabolic engineering to direct carbon toward terpenes (7). The DXS-III gene from *Botryococcus braunii* (15) was cloned and expressed under an IPTG inducible promoter *P*lacO1, and integrated into the neutral site II of *S. elongatus* strain L114 genome (16), creating strain L114/dxs. Limonene productivity was further enhanced to 76.3 μg/L/OD/d (*SI Appendix*, Fig. S1). The productivity of L114/dxs was very similar to the maximum limonene productivity from a recent study where a different LS gene and three bottleneck genes (*dxs-ipphp-gpps*) were coexpressed in the cyanobacterium *Anabaena* sp. PCC 7120 (7). The limited productivity increase by stepwise metabolic engineering might be attributed to the inherent metabolic rigidity of terpene pathways. To produce high titer of bioproducts in microbes, high-flux pathways (17) are desirable to direct sufficient carbon into target compounds. A few studies have implemented primary metabolic pathways to reach a high yield of bioproducts in cyanobacteria (3, 18, 19). In contrast, the MEP pathway is a secondary metabolic pathway with a low carbon partition, believed to be 1% or less (1). Enhancing the carbon partition into the MEP pathway thus requires an understanding of the metabolic network to overcome pathway rigidity.

LS Is a Key Flux-Controlling Node in MEP-Derived Limonene Production

The marginal productivity increase revealed limitations of applying stepwise metabolic engineering strategy on complex pathways such as MEP-derived terpene biosynthesis. Computational simulation could bypass limitations in experimental design, and identify key flux-controlling node in a complex metabolic pathway. We thus conducted a computational modeling study to evaluate how enhanced carbon input to MEP pathway would impact the limonene flux. The computational modeling suggested LS as a major metabolic bottleneck for increasing limonene yield. When the baseline or lower LS kinetics were used in the simulation, enhanced carbon input did not lead to an obvious increase in the limonene flux, indicating major bottlenecks existing in the MEP and/or downstream terpene pathways (Fig. 1*B*). We further simulated the effects of increased LS activity on the limonene flux. Interestingly, enhanced limonene flux was observed following increased carbon input when higher LS activity was used. Particularly, terpene production had a nearly linear response to carbon input when LS activity was increased to 100-fold of the baseline level. Moreover, further enhancing LS activity to 1,000-fold did not lead to limonene flux increase, indicating a saturated MEP flux (Fig. 1*B*). We hypothesize that failure of producing a high

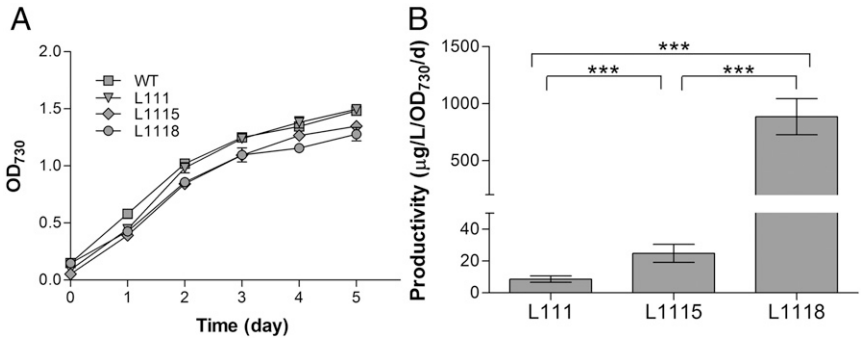

Fig. 2. Enhanced limonene production by strengthening limonene synthase (LS) carbon sink capacity. (*A*) Growth of wild-type and engineered cyanobacterial cells. (*B*) Average limonene productivity in engineered cyanobacterial cells. L111: LS expression driven by *P*trc promoter; L1115: LS expression driven by *S. elongatus* native promoter encoding gene Hbs (Synpcc7942_2248); L1118: LS expression driven by *P*psbA promoter with a synthetic RBS. Error bars indicate the SD of six measurements from 2-d biological triplicates. The two-tailed *t* test showed that all three groups (L111 vs. L1115, L111 vs. L1118, and L1115 vs. L1118) had significant differences with *P* values of <0.0001 (indicated by ***).

yield of terpenes in cyanobacteria could result from low efficiency in terpene synthases to establish a strong carbon sink.

We implemented various strategies to enhance downstream LS expression to experimentally test the computational modeling results. An important approach to enhance heterologous gene expression is to identify and use strong native constitutive promoters. A recent study used a protein fusion strategy to drive β-phellandrene expression in *Synechocystis* by the native *cpc* operon promoter, and enhanced the phellandrene production significantly (20). We identified several potential promoters under which *S. elongatus* proteins expressed at high levels based on proteomics analysis. These potential promoters were used for LS expression and showed various levels of limonene production in engineered cyanobacteria. For example, when LS was driven by the predicted promoter of a gene encoding protein Hbs (Synpcc7942_2248), the strain (L1115) had a limonene productivity of 24.8 μg/L/OD/d (Fig. 2 and *SI Appendix*, File S1), similar to the level reached in strain L113 (*P*trc:*ls*; synthetic RBS). Despite the efforts, it seemed that endogenous promoters failed to enhance the protein expression to a level to overcome the bottleneck indicated by computational modeling. To fully explore the limonene sink capacity, we went to seek promoters that had been validated in cyanobacteria for efficient heterologous gene expression. The pea *psbA* promoter was proved to be highly efficient for ethylene production in *Synechocystis* (21). We thus tested this promoter with a slightly varied RBS (*SI Appendix*, File S1) for LS expression. The result was striking that limonene productivity of strain L1118 increased to an average productivity of 885.1 μg/L/OD/d without any negative impact on growth (Fig. 2). The limonene productivity in L1118 had over 30-fold increase compared with L1115, and over 100-fold increase compared with the initial L111 line. The proteomics analysis also verified the increased expression of LS in L1118 line. Compared with L1115, LS abundance increased over 13-fold in L1118 (*SI Appendix*, Fig. S3 and Dataset S1). Interestingly, *S. elongatus* genome does not encode a homologous GPPS to synthesize geranyl pyrophosphate, the substrate for LS. Instead, a farnesyl pyrophosphate synthase (Synpcc7942_0776) could be multifunctional and be used as the first enzyme to condense IPP and DMAPP into C_{10} terpene precursors, considering the high limonene productivity achieved without introducing exogenous GPPS. The experimental data successfully validated the computational modeling results, and revealed that LS is a key metabolic node to enhance terpene flux. By enhancing this key flux-controlling node, we achieved a high productivity for limonene production in cyanobacteria, and over 10-fold increase compared with the maximum productivity in a recent study with multiple pathway genes engineered (7). Computational modeling coupled with synthetic biology-based engineering thus provides a powerful tool to identify key carbon flux-controlling nodes in various metabolic pathways. Understanding how these nodes are regulated in a larger metabolic network will bring valuable information on carbon partition, and further guide metabolic engineering efforts.

Synergy Between Photosynthesis and Downstream Limonene Biosynthesis

With the establishment of a strong limonene flux, we conducted a proteomics study to analyze metabolism changes between *S. elongatus* wild type and L1118. Compared with wild type, many ribosomal proteins and chaperons were found in higher abundance in L1118 line (Fig. 3*A* and Dataset S1), which could be explained by the increased protein translation and turnover rate to generate LS and other enzymes. Moreover, the majority of proteins accumulated in the limonene line L1118 belong to those involved in photosynthesis metabolism (Fig. 3). Several enzymes in the Calvin–Benson–Bassham (CBB) cycle had translational regulation. A subunit of ribulose 1,5-bisphosphate carboxylase/oxygenase (RuBisCO) in the carbon fixation stage of CBB cycle, phosphoglycerate kinase

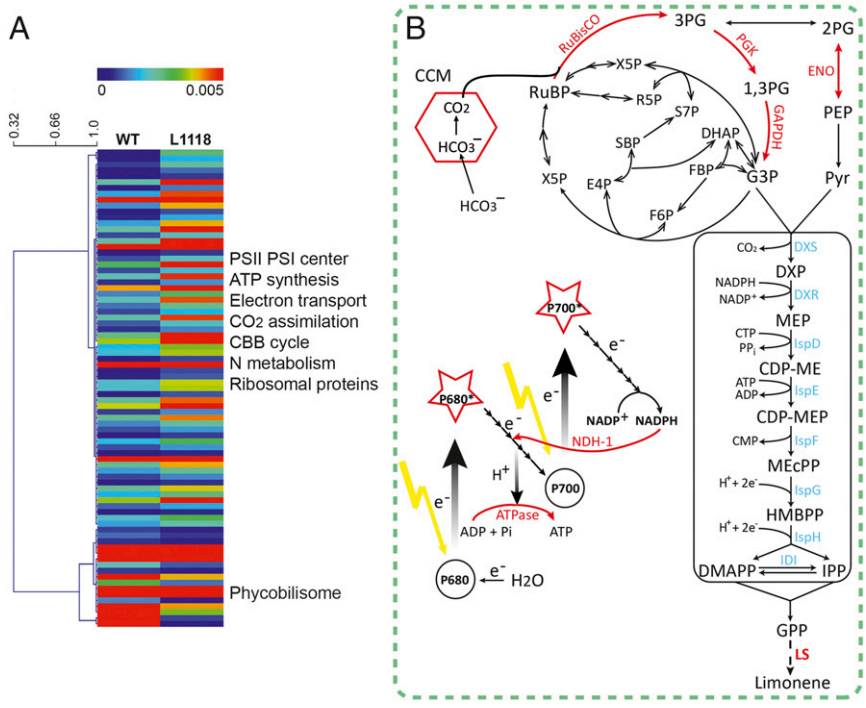

Fig. 3. Proteomics analysis of *S. elongatus* wild-type and L1118 cells. (*A*) Heat map showing differentially expressed proteins in WT and L1118 cells. Up-regulated and down-regulated proteins in L1118 were categorized into their relative metabolism (for full protein identities, see Dataset S1). (*B*) Up-regulated proteins in L1118 were labeled in red, and mapped into pathways. The majority of these proteins were found belonging to photosynthesis metabolism including both light and dark reactions. ATPase subunits (three subunits encoded by genes atpC, atpF, and atpA); NDH-1 (NAD(P)H-quinone oxidoreductase subunit O and subunit I); RuBisCO, ribulose-1,5-bisphosphate carboxylase/oxygenase; PGK, phosphoglycerate kinase; GAPDH, glyceraldehyde 3-phosphate dehydrogenase; ENO, enolase.

(PGK), and glyceraldehyde 3-phosphate dehydrogenase (GAPDH) (encoded by *gap2*) in the carbon reduction stage of CBB cycle were all up-regulated, potentially leading to enhanced CBB cycle efficiency and increased G3P generation. A previous study showed that carbon partition between carbon fixation and pyruvate generation could be altered through manipulating 3-phophoglycerate (3PG) catabolic enzymes (22). In the L1118 line, enolase from the 3PG catabolic pathway was also found in higher abundance, which could lead to enhanced pyruvate generation from 3PG (Fig. 3*B* and Dataset S1). The concurrent up-regulation of G3P and pyruvate-generating enzymes suggests enhanced carbon input into the MEP pathway to support limonene biosynthesis.

In addition, a cell absorbance spectral scan showed that L1118 cells had a reduced amount of phycobilin, whereas chlorophyll *a* and carotenoid contents were unaltered (Fig. 4*A*). This observation corroborates proteomics results, in which the majority of down-regulated proteins in L1118 belonged to phycobilisome (PBS) components, ranging from 1.8- to over 20-fold decrease in abundance (Fig. 3*A* and Dataset S1). Because IPP and DMAPP can also be used for the synthesis of chlorophyll and carotenoid, their unaltered contents further indicate that limonene flux increase was from enhanced MEP flux rather than precursor redistribution. These results revealed potential synergy between photosynthate output and downstream limonene biosynthesis, and indicated enhanced carbon flux into the MEP pathway through upstream photosynthetic regulations.

Evolutionally speaking, biomass accumulation has evolved as the native photosynthesis carbon sink. A "nonnative" carbon sink has the potential to enhance photosynthesis, and drive bioproduct production. Indeed, ethylene-producing cyanobacteria diverted over 5% fixed carbon to ethylene, surpassing carbon partition into the tricarboxylic acid (TCA) cycle (21). Enhanced carbon fixation was also observed in sucrose-exporting cyanobacteria (19). An efficient terpene carbon sink would have enormous applications, provided photosynthesis could support the terpene production.

Photosynthesis Limitations in Enhancing Limonene Production

To reflect the photosynthesis activity during limonene production, we measured the whole cell O_2 evolution in wild type and L1118. Surprisingly, L1118 limonene cells showed a relatively slower photosynthesis efficiency compared with wild-type cells (Fig. 4*B*). A closer look at the proteome led us to think the slower O_2 evolution in L1118 could be caused by electron halt in the electron transport chain. We first noticed the increased level of protein CP12 in L1118 cells (Dataset S1). CP12 can reversibly bind phosphoribulokinase (PRK) and GAPDH to form a large PRK/CP12/GAPDH protein complex to regulate the CBB cycle (23). In *S. elongatus*, the association/dissociation of the PRK/CP12/GAPDH protein complex was found to be dependent on the ratio of NAD(H)/NADP(H), in which NADPH could bind with CP12 and release PRK from the complex to enhance PRK activity (24). The increased CP12 level could indicate the accumulation of NADPH in L1118, leading to increased free subunits of CP12. The measurement of NADPH confirmed this hypothesis as NADPH levels were higher in L1118 during limonene production (Fig. 4*C*). NADPH accumulation limits the availability of terminal electron acceptor for photosynthesis, leading to slower electron flow in photosynthesis light reaction (4), thus slower O_2 evolution. Interestingly, certain photosystem II (PSII) and photosystem I (PSI) subunits proteins were found in higher abundance in the L1118 line. We found PSII protein Psb28 increased threefold in the L1118 limonene line (Dataset S1). Psb28 is involved in biosynthesis of PSII chlorophylls and structurally associated with PSII inner antenna CP47 in *Synechocystis* PCC6803 (25). PsaD, a peripheral protein of PSI on the stromal side playing major roles in both the function and assembly of PSI (26), had over twofold increase in L1118. In addition, a certain cytochrome b_6f complex subunit, and NAD(P)H-quinone oxidoreductase subunits were also found in higher abundance in L1118 cells (Dataset S1). These increased proteins all belong to protein complexes involved in photosynthetic light reaction. Considering that we saw a decrease in O_2 evolution, it is likely that the increased subunits are not functionally assembled in the active protein complex, instead existing as free subunits. In addition, higher NADPH level might be linked to the decreased phycobilin in

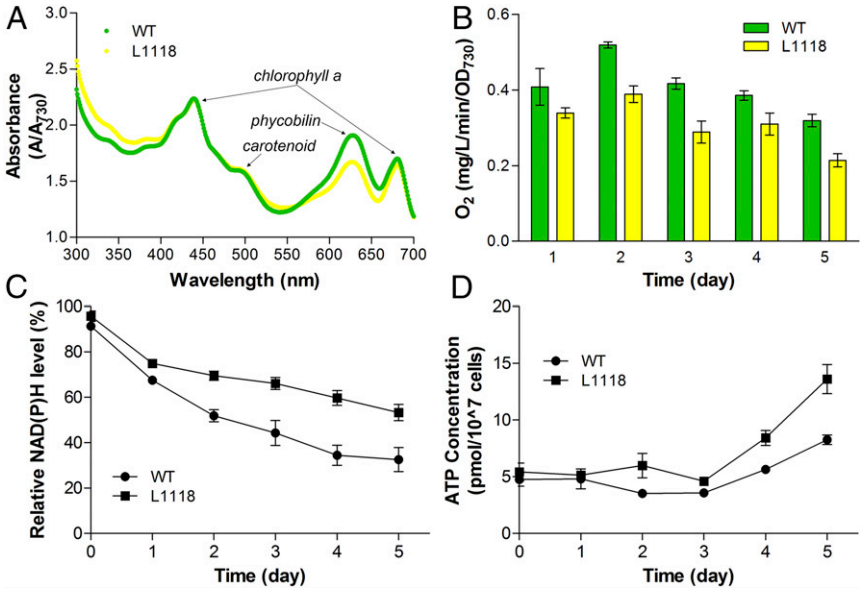

Fig. 4. Photosynthesis efficiency and energy requirement during limonene production. (*A*) Whole-cell absorbance spectra of WT and L1118 cells. The absorption peaks for different pigments were indicated. (*B*) O_2 evolution rate for WT and L1118. The paired *t* test showed a significant difference between WT and L1118 with a *P* value of 0.0014 (<0.01). (*C*) NADPH measurement by spectrofluorometer (Ex 340 nm; Em 460 nm) for WT and L1118 cells. The paired *t* test showed a significant difference between WT and L1118 with a *P* value of 0.0051 (<0.01). (*D*) ATP measurement of WT and L1118 cells. The paired *t* test showed no significant difference between WT and L1118 with a *P* value of 0.04 (> 0.01). Error bars indicate the SD.

L1118, because NADPH accumulation could lead to overreduction of plastoquinone pool and photoinhibition (27), which can potentially lead to PBS degradation to protect cells from photoinhibition (27).

To further elucidate changes in photosynthesis light reaction, we measured the ATP contents in both wild-type and L1118 cells. ATP level was found at similar levels during log-phase growth of wild-type and L1118 cells, but both cell lines accumulated ATP when cells entered stationary phase (Fig. 3*D* and *SI Appendix*, Fig. S4). However, the paired *t* test showed no significant differences between wild-type and L1118 cells. Considering NADPH accumulation throughout the growth, it seems that efficient limonene production requires a lower ratio of ATP/NADPH. This observation is in agreement with a previous modeling study which revealed the lower ATP/NADPH ratio requirement for many biofuel molecules (28). In photosynthesis light reaction, linear electron flow is believed to produce ATP/NADPH in a ratio of approximately 1.28/1 (4). Biomass accumulation is believed to require ATP/NADPH in a ratio of at least 1.51/1 (29), in which additional ATP is supplied by alternative electron flows (4). However, a nonnative carbon sink usually lacks the pathway complexity, and requires a smaller ATP/NADPH ratio compared with biomass accumulation (28). The photosynthesis light reaction thus might not require additional stimulation to accommodate the energy needs in these nonnative carbon sinks. Our results suggest a lower ATP/NADPH ratio requirement in MEP-derived limonene biosynthesis, leading to an imbalance of ATP/NADPH production and consumption.

In conclusion, LS was identified as a key metabolic flux-controlling node in enhancing cyanobacterial limonene flux. We successfully tackled this problem and created a strong limonene sink in cyanobacteria. However, the still-elusive MEP pathway regulation (30) presents further obstacles in directing sufficient carbon to downstream terpene synthesis. More importantly, we show that the strong limonene sink led to NADPH accumulation and slowed down photosynthesis electron flow. Fine-tuning the ATP/NADPH ratio could be an important direction to modulate photosynthesis to support the production of biofuel/bioproducts. Enhancing photosynthesis to support terpene production is key to realize an efficient cyanobacterial terpene platform.

Materials and Methods

Growth Conditions. *S. elongatus* wild-type and engineered strains were grown in BG11 medium (Sigma) supplemented with 10 mM *N*-[Tris(hydroxymethyl)methyl]-2-aminoethanesulfonic acid (TES, pH 8.2) at 30 °C. Unless indicated otherwise, cells grown in the 1-L Roux bottle were aerated with 5% (vol/vol) CO_2 under 100-μmol photons $m^{-2}{\cdot}s^{-1}$ illumination from cool white fluorescent lamps. Seed cultures were grown in 250-mL Erlenmeyer flasks in BG11 medium supplemented with 20 mM $NaHCO_3$ and 10 mM TES under 50-μmol photons m^{-2} s^{-1} illumination. Engineered strains were grown with the addition of 2 mg/l spectinomycin/streptomycin (neutral site I targeting strains) and/or 5 mg/l kanamycin (neutral site II targeting strains). Details of strain information are available in *SI Appendix, SI Methods*.

Limonene Collection and Measurement by Gas Chromatography–Mass Spectrometry. The hydrophobicity and high vapor pressure of limonene enabled in situ product collection by a hydrocarbon absorbent trap coupled to the photobioreactor. Cyanobacterial cells (500 mL) were grown in triplicates in 1-L Roux bottle coupled with a HayeSep porous polymer absorbent (Sigma) to trap limonene. The trap was collected each day, and limonene was eluted with 1 mL hexane supplemented with 10 μg/mL cedrene (Sigma) as the internal standard. One μL of the eluted sample was analyzed by gas chromatography–mass spectrometry (GC-MS) (Shimadzu Scientific Instruments, Inc.). The sample was injected into a Shimadzu SH-Rxi-5Sil column (30 m × 250 μm × 0.25 μm) with a helium flow rate of 1.0 mL/min. The GC program was set as follows: 40 °C hold for 3 min, followed by temperature increase to 140 °C at the rate of 20 °C/min, and finally to 300 °C at the increment of 25 °C/min. Limonene concentration was calculated based on a standard curve established with known limonene concentrations. The final limonene yield was adjusted by the trap recovery rate, which was determined by supplementing 500 mL of *S. elongatus* wild-type cells with various concentrations of limonene. Limonene was collected the next day following the same procedure described above, and a standard curve was generated to calculate the limonene recovery (*SI Appendix*, Fig. S5). The average limonene productivity was calculated from a 2-day limonene production during the log-phase cell growth.

O_2 Evolution. Two mL of both wild-type and limonene-producing cells from biological triplicates were collected each day for photosynthesis activity measurement following the previously described method (31). Briefly, cells were pelleted and resuspended in the TES buffer (20 mM TES; 100 mM $NaHCO_3$, and 230 μM K_2HPO_4). The O_2 evolution rate was measured at room temperature with saturated light (1,000 μE $m^{-1}{\cdot}s^{-1}$) using a dissolved oxygen cuvette electrode equipped with light-emitting diode light source (Qubit Systems).

ATP Extraction and Measurement. Cyanobacterial cells (1.5 mL) from biological triplicates were collected each day. Cell pellets were collected by centrifugation at 13,000 rpm for 3 min, followed by resuspension in 100 μL 1% ice-cold trichloroacetic acid solution. After vortexing for 30 s in 1% trichloroacetic acid, the supernatant was collected by centrifuging at 13,000 rpm for 10 min at 4 °C. One hundred μL 1 M Tris-Acetate buffer (pH 7.8) was used to neutralize the trichloroacetic acid solution. The ATP-containing solution was further diluted to 1 mL with deionized water. Ten μL of the ATP solution was used to measure the ATP content using the ATP determination kit (Molecular Probes Inc.) following manufacturer's instructions. ATP concentration was calculated from a standard curve prepared together with the sample measurement.

NADPH Measurement. Biological triplicates of 500 mL of *S. elongatus* wild-type and limonene-producing cells were grown with 5% (vol/vol) CO_2 under 100-μmol photons $m^{-2}{\cdot}s^{-1}$ illumination. Three mL of cells were collected each day and used for NADPH measurement using a FluoroMax-4 spectrofluorometer (HORIBA Scientific). Wild-type and limonene cells were excited at 340 nm, and fluorescence signal was collected over the range of 350–550 nm. Because pyrimidine contents consist of mainly NADPH in *S. elongatus* (24), the maximum fluorescence emission for NAD(P)H (460 nm) (32) was normalized by cell density (OD_{730}), and used to compare NADPH contents between wild-type and limonene cells.

Kinetics Modeling. See *SI Appendix, SI Methods*.

Proteomics Sample Preparation and Data Analysis. See *SI Appendix, SI Methods*. The mass spectrometry proteomics data have been deposited to the ProteomeXchange Consortium via the PRIDE (33) partner repository with the dataset identifier PXD005105.

ACKNOWLEDGMENTS. We thank Haijun Liu (Washington University in St. Louis) for the careful reading of the manuscript and valuable input. Special thanks to Jianping Yu (National Renewable Energy Laboratory) and James Golden (University of California, San Diego) for their plasmids. We thank Samantha Kristufek (Texas A&M University) for technical training with the fluorescence spectrophotometer. We thank Cheng Hu, Cheng Zhao, and Zhaoren He for help in preparing media and conducting plasmid extractions. This work was supported by Grant DOE-ARPA-E-PETRO DE-AR0000203 to J.S.Y., S.Y.D., and X.Z.; the Welch Foundation Support Grant 1501928 to P.M.R.; Texas A&M AgriLife Seed Grant to J.S.Y., S.Y.D., P.M.R., and X.W.; and Texas A&M Engineering Experiment Station.

1. Melis A (2013) Carbon partitioning in photosynthesis. *Curr Opin Chem Biol* 17(3):453–456.
2. Wang X, Ort DR, Yuan JS (2015) Photosynthetic terpene hydrocarbon production for fuels and chemicals. *Plant Biotechnol J* 13(2):137–146.
3. Xiong W, et al. (2015) The plasticity of cyanobacterial metabolism supports direct CO_2 conversion to ethylene. *Nat Plants* 1:15053.
4. Kramer DM, Evans JR (2011) The importance of energy balance in improving photosynthetic productivity. *Plant Physiol* 155(1):70–78.
5. Formighieri C, Melis A (2014) Regulation of β-phellandrene synthase gene expression, recombinant protein accumulation, and monoterpene hydrocarbons production in *Synechocystis* transformants. *Planta* 240(2):309–324.
6. Halfmann C, Gu L, Gibbons W, Zhou R (2014) Genetically engineering cyanobacteria to convert CO_2, water, and light into the long-chain hydrocarbon farnesene. *Appl Microbiol Biotechnol* 98(23):9869–9877.
7. Halfmann C, Gu L, Zhou R (2014) Engineering cyanobacteria for the production of a cyclic hydrocarbon fuel from CO_2 and H_2O. *Green Chem* 16(6):3175–3185.
8. Hyatt DC, et al. (2007) Structure of limonene synthase, a simple model for terpenoid cyclase catalysis. *Proc Natl Acad Sci USA* 104(13):5360–5365.
9. Williams DC, McGarvey DJ, Katahira EJ, Croteau R (1998) Truncation of limonene synthase preprotein provides a fully active 'pseudomature' form of this monoterpene cyclase and reveals the function of the amino-terminal arginine pair. *Biochemistry* 37(35):12213–12220.
10. Ivleva NB, Bramlett MR, Lindahl PA, Golden SS (2005) LdpA: A component of the circadian clock senses redox state of the cell. *EMBO J* 24(6):1202–1210.
11. Salis HM, Mirsky EA, Voigt CA (2009) Automated design of synthetic ribosome binding sites to control protein expression. *Nat Biotechnol* 27(10):946–950.
12. Wu S, et al. (2006) Redirection of cytosolic or plastidic isoprenoid precursors elevates terpene production in plants. *Nat Biotechnol* 24(11):1441–1447.

13. Burke C, Croteau R (2002) Geranyl diphosphate synthase from Abies grandis: cDNA isolation, functional expression, and characterization. *Arch Biochem Biophys* 405(1):130–136.
14. Wright LP, et al. (2014) Deoxyxylulose 5-Phosphate synthase controls flux through the methylerythritol 4-phosphate pathway in *Arabidopsis*. *Plant Physiol* 165(4):1488–1504.
15. Matsushima D, et al. (2012) The single cellular green microalga *Botryococcus braunii*, race B possesses three distinct 1-deoxy-D-xylulose 5-phosphate synthases. *Plant Sci* 185-186:309–320.
16. Andersson CR, et al. (2000) Application of bioluminescence to the study of circadian rhythms in cyanobacteria. *Methods Enzymol* 305:527–542.
17. Jeong H, Tombor B, Albert R, Oltvai ZN, Barabási AL (2000) The large-scale organization of metabolic networks. *Nature* 407(6804):651–654.
18. Atsumi S, Higashide W, Liao JC (2009) Direct photosynthetic recycling of carbon dioxide to isobutyraldehyde. *Nat Biotechnol* 27(12):1177–1180.
19. Ducat DC, Avelar-Rivas JA, Way JC, Silver PA (2012) Rerouting carbon flux to enhance photosynthetic productivity. *Appl Environ Microbiol* 78(8):2660–2668.
20. Formighieri C, Melis A (2015) A phycocyanin·phellandrene synthase fusion enhances recombinant protein expression and β-phellandrene (monoterpene) hydrocarbons production in *Synechocystis* (cyanobacteria). *Metab Eng* 32:116–124.
21. Ungerer J, et al. (2012) Sustained photosynthetic conversion of CO_2 to ethylene in recombinant cyanobacterium *Synechocystis* 6803. *Energy Environ Sci* 5(10):8998–9006.
22. Oliver JW, Atsumi S (2015) A carbon sink pathway increases carbon productivity in cyanobacteria. *Metab Eng* 29:106–112.
23. Wedel N, Soll J, Paap BK (1997) CP12 provides a new mode of light regulation of Calvin cycle activity in higher plants. *Proc Natl Acad Sci USA* 94(19):10479–10484.
24. Tamoi M, Miyazaki T, Fukamizo T, Shigeoka S (2005) The Calvin cycle in cyanobacteria is regulated by CP12 via the NAD(H)/NADP(H) ratio under light/dark conditions. *Plant J* 42(4):504–513.
25. Dobáková M, Sobotka R, Tichý M, Komenda J (2009) Psb28 protein is involved in the biogenesis of the photosystem II inner antenna CP47 (PsbB) in the cyanobacterium *Synechocystis* sp. PCC 6803. *Plant Physiol* 149(2):1076–1086.
26. Lagoutte B, Hanley J, Bottin H (2001) Multiple functions for the C terminus of the PsaD subunit in the cyanobacterial photosystem I complex. *Plant Physiol* 126(1):307–316.
27. Salomon E, Bar-Eyal L, Sharon S, Keren N (2013) Balancing photosynthetic electron flow is critical for cyanobacterial acclimation to nitrogen limitation. *Biochimica et Biophysica Acta (BBA) -. Bioenergetics* 1827(3):340–347.
28. Kämäräinen J, et al. (2012) Physiological tolerance and stoichiometric potential of cyanobacteria for hydrocarbon fuel production. *J Biotechnol* 162(1):67–74.
29. Erdrich P, Knoop H, Steuer R, Klamt S (2014) Cyanobacterial biofuels: New insights and strain design strategies revealed by computational modeling. *Microb Cell Fact* 13:128.
30. Banerjee A, Sharkey TD (2014) Methylerythritol 4-phosphate (MEP) pathway metabolic regulation. *Nat Prod Rep* 31(8):1043–1055.
31. Carrieri D, Paddock T, Maness PC, Seibert M, Yu JP (2012) Photo-catalytic conversion of carbon dioxide to organic acids by a recombinant cyanobacterium incapable of glycogen storage. *Energy Environ Sci* 5(11):9457–9461.
32. Blacker TS, et al. (2014) Separating NADH and NADPH fluorescence in live cells and tissues using FLIM. *Nat Commun* 5:3936.
33. Vizcaíno JA, et al. (2016) 2016 update of the PRIDE database and its related tools. *Nucleic Acids Res* 44(D1):D447–D456.